2012

Performance of Permutation Trellis Codes in Cognitive Radio Networks

Raghed El Bardan
Syracuse University

Engin Masazade
Syracuse University

Onur Ozdemir
ANDRO Computational Solutions

Pramod Varshney
Syracuse University, varshney@syr.edu

Recommended Citation

R. E. Bardan, E. Masazade, O. Ozdemir, and P. K. Varshney, "Performance of Permutation Trellis Codes in Cognitive Radio Networks," in 2012 35th IEEE Sarnoff Symposium, 21-22 May 2012, Piscataway, NJ, USA, 2012, p. 6 pp.

Performance of Permutation Trellis Codes in Cognitive Radio Networks

Raghed El Bardan*, Engin Masazade*, Onur Ozdemir†, and Pramod K. Varshney*
* Department of EECS, Syracuse University, NY 13244, {raelbard,emasazad, varshney}@syr.edu
† ANDRO Computational Solutions, LLC, 7902 Turin Road, Rome, NY 13440, oozdemir@androcs.com.

***Abstract*—In this paper, we investigate the error correction performance of Permutation Trellis Codes (PTC) combined with M-ary Frequency Shift Keying (M-FSK) modulation in Cognitive Radio Networks (CRNs). Using this modulation technique, a secondary user (SU) can improve its data rate by increasing its transmission bandwidth while operating at low power and without creating destructive interference to the primary users (PUs). Given an active PU, we first derive the bit error rate (BER) of the PTC based M-FSK system for a given SU link. For different PTCs, we compare the analytical BER with the corresponding simulation results. For the same transmitting power, bandwidth availability and transmission time, simulation results show that for a SU link, M-FSK scheme using PTC provides better protection against the interference caused by the PU than M-FSK schemes employing conventional error correction coding such as convolutional and low density parity check (LDPC) codes.**

I. Introduction

Today, a large portion of the frequency spectrum assigned by the Federal Communications Commission (FCC) is used intermittently resulting in spectrum scarcity and inefficient usage of the assigned frequency bands. In this context, Cognitive Radios (CRs) have been presented as the new communication paradigm for wireless systems utilizing the existing spectrum opportunistically [1], [2]. Primary users are the licensed users who have the right to access their spectrum at any time. In a cognitive radio network, secondary users detect the spectrum holes which are the frequency bands not used by primary users and transmit over them [3], [4]. Secondary users can also coexist with the primary users at the same time as long as secondary users do not violate the quality of service requirements of the primary users [5], [6]. Orthogonal frequency division multiplexing (OFDM) has been suggested as a multi-carrier communication candidate for CR systems where the available spectrum is divided into sub-carriers each of which carries a low rate data stream [7], [8], [9], [10], [11]. Typically, in CRNs, an SU senses the PU activity of the channel and adjusts its communication parameters accordingly. Conversely, whenever a PU stops transmission and another PU joins the network over a different frequency band, the SU needs to re-sense the channel and adapt its transmission parameters. Hence, continuous spectrum sensing and reformation of wireless links may result in substantial performance degradation of the SUs.

In this paper, we propose a new communication scheme based on M-ary Frequency Shift Keying (M-FSK) for CRNs. This kind of orthogonal signalling is power limited and requires a large bandwidth to provide high data rates [12]. Since the frequency spectrum allocated for the usage of SUs is assumed to be large in CRNs, an SU can function with low power without degrading the performance of an ongoing PU activity and increase its data rate by increasing its bandwidth. On the other hand, whenever a PU becomes active on a frequency band that the SU is operating on, it creates interference and severely degrades the SU link quality. We assume that an SU can transmit on a frequency band where the PU is active on the condition that the performance of the ongoing PU communication is not degraded. Therefore, the SU needs powerful error correction codes to mitigate the interference created by the PUs.

Error correction coding (ECC) has been proposed for CRNs in the literature. In [8], the authors assume that an SU transmitter vacates the band in CRNs once a PU is detected. Due to the sudden appearance of a PU, rateless codes have been considered to compensate for the packet loss in secondary data which is transmitted through parallel subchannels. The authors in [9], consider the design of two efficient anti-jamming coding techniques for lost transmitted packets recovery via parallel channels, namely rateless and piecewise coding. Similar to the spectrum model defined in [8], the system's throughput and goodput are analyzed and a performance comparison is done between these two coding techniques. For an OFDM-based CRN presented in [10], the SU transmitter and receiver continuously sense the spectrum, exchange information and decide on the available and unavailable portions of the frequency spectrum. Depending on the frequency availability, an appropriate Reed-Solomon coding scheme is used to retrieve the bits transmitted over the unavailable portions of the frequency spectrum. The authors in [11] further explore LDPC codes in an OFDM scheme to correct the bits received in error where a switching model was considered for dynamic and distributed spectrum allocation as well as analyze the effects of varied PU detection performance. The switch is assumed to be open for each cognitive user detecting a primary user. When the switch is open, the channel is modeled as a binary erasure channel (BEC) and the cognitive transmitter continues to transmit its message allowing bits to be erroneous when received. Another major use of the ECC schemes is presented in [13] where the authors study the performance of cooperative relaying in cognitive radio networks using rateless coding error-control mechanism. They assume that an SU transmitter participates in PU's transmission as a relay instead of vacating the band in order to reduce the channel access time by a PU. Since the use of rateless codes allows the SU receiver to decode data regardless of which packets it has received as long as enough number of encoded packets are received, these codes are very suitable for cooperative schemes. Ao and Chen in [14] propose an end-to-end hybrid ARQ scheme in CRNs consisting of unidirectional opportunistic links to reduce the number of retransmissions with a fixed throughput offset. Their error control approach is based on coded cooperation among paths and amplify-and-forward relaying of packets within a path such that this hybrid ARQ works for CRNs even if some coded data are missing. The authors implement their scheme using convolutional codes combined with BPSK modulation.

In this paper, we investigate the error correction performance of Permutation Trellis Codes (PTC) [15], [16] combined with M-ary Frequency Shift Keying (M-FSK) modulation to overcome the effect of PU interference on an SU transmission. In our model, an SU can transmit its own information concurrently with PU transmissions without the need to relay PU's traffic [13] or vacate the band [8]. Different from [10], we assume that no information exchange or spectrum negotiation takes place between the SU transmitter receiver pair. Our proposed scheme is different from existing work where transmission is carried over parallel subchannels [8], [9], [10], [11]. This is due to the fact that our scheme is based on M-FSK modulation with PTC using a single subchannel at a time. By using PTC, continuous channel sensing of the SU transmitter receiver pair is no longer required since an appropriate PTC code can cope with a certain number of PU interferences on a given SU link. Given PU activity, we first derive the bit error rate (BER) for an SU link. Derivation of BER for a given SU link is important since it can be used as a metric to determine a given SU link quality which has not been considered in the schemes [8], [10], [11], [9], [13], [14], [17]. Moreover, the BER of a PTC based communication system has not been provided in [15], [16]. We further verify the analytically derived BER with simulation results and show that M-FSK signalling with PTC coding provides superior performance compared to the conventional M-FSK schemes using convolutional or LDPC coding.

The rest of the paper is organized as follows: In Section II, we provide the system model, introduce the concept of PTC, and derive the analytical expression of average symbol error probability P_s. Section III presents numerical examples to demonstrate the effectiveness of the proposed communication scheme. Finally, Section IV concludes the paper and addresses some future research directions.

II. System Model

We consider a simple cognitive radio network as shown in Fig. 1, which consists of a PU transmitter-receiver pair and an SU transmitter-receiver pair. The SU pair is located within the transmission range of the PU. The transmission range shown in Fig. 1 is the maximum distance covered by a PU transmission such that the signal to interference plus noise ratio (SINR) at the PU receiver equals a minimum threshold value, $SINR^*_{PU}$.

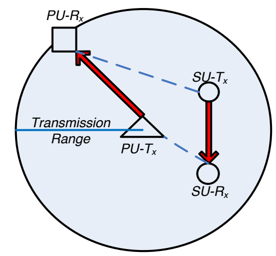

Fig. 1: A simple cognitive radio network.

In this model, we assume a free space path loss model and a Line-Of-Sight (LOS) channel. The power in the transmitted signal is P_t, so the received power is:

$$P_r = P_t \cdot \left(\frac{\sqrt{G_l}\lambda}{4\pi d} \right)^2 \quad (1)$$

where $\sqrt{G_l}$ is the product of the transmit and receive antenna field gains in LOS direction and λ, is the signal wavelength defined as the ratio of the speed of light to the center frequency of the band in operation, $\frac{C}{f_j}$. In this model, we assume omnidirectional antennas so $\sqrt{G_l} = 1$. Both licensed and unlicensed users coexist and can simultaneously operate over the same band. One further assumption made here is that interference, created by an SU, that deteriorates the QoS of the PU is negligible compared to the received PU power. This is due to the fact that the transmission power of PU is much larger than the transmission power of SU, i.e., $P_T^{SU} \ll P_T^{PU}$. In other words, the SINR at the PU receiver [18] given in (2) satisfies $SINR \geq SINR^*_{PU}$.

$$SINR = \frac{P_R^{PU}}{N_0 + P_I^{SU}} \approx \frac{P_R^{PU}}{N_0} \quad (2)$$

where P_I^{SU} is the SU interference at the PU receiver.

A. System Description

An overview of the signal processing procedure that combines the PTC scheme with the FSK communication system is provided in Fig. 2. The information bits are serially loaded into a bit-to-symbol convertor that outputs M different symbols. The PTC encoder assigns a certain code matrix for each symbol and the code matrix is transmitted over time and frequency. We consider an example for illustration, in which the symbol '10' is mapped into '213'. This permutation code matrix is to be transmitted in both time and frequency domains resulting in a 3 x 3 (H x H) binary code matrix as given below:

$$\mathbf{T_i} = \begin{bmatrix} 0 & 1 & 0 \\ 1 & 0 & 0 \\ 0 & 0 & 1 \end{bmatrix} \quad (3)$$

where $1 \leq i \leq M$ and H defines the number of frequency bands as well as the number of time steps used in transmitting the outputs of the encoder. According to (3), transmission takes place on f_2, f_1, and f_3 (first, second and third columns

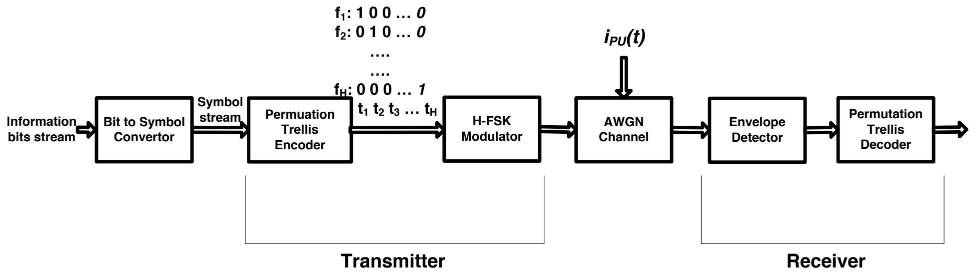

Fig. 2: Signal processing from transmitter to receiver

of $\mathbf{T}_i$) corresponding to the time instants t_1, t_2, and t_3 respectively. Table 1 presents the symbol mappings into a unique permutation code matrix for $m = 2$ [15]. Since the

TABLE I: Mapping of symbols into permutation code matrices

Symbol	Permutation code matrix
00	123
01	132
10	213
11	231

permutation trellis coded FSK modulated system leads to an H x H binary code matrix, we refer to it as the *H-FSK communication system* in this paper.

For $M = 2^m$ symbols, $\mathbf{T}_i$ denotes the set of transmitted code matrices such that $\mathbf{T}_i \in \{\mathbf{T}_1, \ldots, \mathbf{T}_M\}$ and has the following form:

$$\mathbf{T}_i = \begin{bmatrix} q_{1,1} & q_{1,2} & \cdots & q_{1,H} \\ \vdots & \ddots & \cdots & \vdots \\ q_{H,1} & \cdots & \cdots & q_{H,H} \end{bmatrix} \tag{4}$$

where $q_{j,k} \in \{0, 1\}$ denotes the (j, k) binary element in the transmitted code matrix, j indicates the output of the detector for frequency f_j, and k, the position or time in the code matrix. At each time instant, the elements are modulated and transmitted in parallel. Using the H-FSK scheme, the transmitted symbol over j^{th} frequency and k^{th} time step where $j \in \{1, 2, \ldots, H\}$ and $k \in \{1, 2, \ldots, H\}$ is given by:

$$\begin{aligned} s_{j,k}(t) &= \sqrt{2E_s^t/T_s} \cdot \cos(2\pi f_{j,k} t), \quad 0 \le t \le T_s \\ f_{j,k} &= f_1 + \frac{j-1}{T_s}, \quad 2 \le j \le H,\ 1 \le k \le H \end{aligned} \tag{5}$$

where $E_s^t = P_T^{SU} \cdot T_s$ is the transmitted signal energy per modulated symbol and T_s is the symbol duration. Channel noise is modeled as AWGN with zero-mean and variance $N_0/2$. In order to satisfy fixed signal-to-noise ratio, E_b/N_0, for all the received bits, the received signal power over the different frequency channels should be the same as $P_R^{SU}(f_1) = \ldots = P_R^{SU}(f_H) = P_R^{SU}$. In order to satisfy this property, on the transmitter side, we adjust each SU's transmitting power over each frequency, $P_T^{SU}(f_j)$, according to the free space path loss model given in (1). Without loss of generality, we assume that the SU transmitter knows the location of the SU receiver before transmission. At the input of the demodulator, the received signal is given by:

$$x_j(t) = \begin{cases} s_j^r(t) + i_{PU}^r(t) + w(t) & \text{if PU exists on } f_j \\ s_j^r(t) + w(t) & \text{otherwise} \end{cases}$$

where $s_j^r(t) = \sqrt{2\frac{E_s^r}{T_s}}\cos(2\pi f_j t + \theta)$ and $i_{PU}^r(t) = \sqrt{2\frac{I_{PU}}{T_s}}\cos(2\pi f_j t + \phi)$ where $E_s^r = P_R^{SU} T_s$ is defined as the symbol energy at the receiver. $I_{PU} = P_I^{PU} T_s$ and P_I^{PU} are defined as the interference energy per symbol and the interference power of the PU transmitter to the SU receiver respectively.

At the receiver side, non-coherent detection is employed using a bank of H quadrature receivers so that each consists of two correlation receivers corresponding to in-phase and quadrature components of the signal. The in-phase component of the signal received, $x_{I_{j,k}}$, is given by:

$$x_{I_{j,k}} = \begin{cases} E_s^r \cos\theta + I_{PU}\cos\phi + w & \text{if PU exists on } f_j \text{ at time } k \\ E_s^r \cos\theta + w & \text{otherwise} \end{cases}$$

where θ, $\phi \sim U(0, 2\pi)$ denote the random phase components of the SU and the PU signals respectively, and $w \sim N(0, \frac{N_0}{2})$. On the other hand, $x_{Q_{j,k}}$ is the received signal's quadrature component. It is defined as follows:

$$x_{Q_{j,k}} = \begin{cases} E_s^r \sin\theta + I_{PU}\sin\phi + w & \text{if PU exists on } f_j \text{ at time } k \\ E_s^r \sin\theta + w & \text{otherwise} \end{cases}$$

The envelope of each quadrature receiver over frequency j and time step k, $l_{j,k}$, is defined as the square root of the sum of the squared in-phase and quadrature components of the correlator output as,

$$l_{j,k} = \sqrt{x_{I_{j,k}}^2 + x_{Q_{j,k}}^2} \tag{6}$$

Each envelope at the output of H quadrature receivers is compared to a threshold value, l_{th}. The threshold value we use in our derivation is the same as used by the authors in [15], namely $l_{th} = 0.6\sqrt{E_s}$. Let $b_{j,k}$ denote the binary output of the quadrature receiver. For values above the threshold, the quadrature receiver output $b_{j,k} = 1$, otherwise, $b_{j,k} = 0$. The received code matrix $\mathbf{R}_n$ where $n \in \{1,\ldots,2^{H^2}\}$ is of the following form:

$$\mathbf{R}_n = \begin{bmatrix} b_{1,1} & b_{1,2} & \ldots & b_{1,H} \\ \vdots & \ddots & \ldots & \vdots \\ b_{H,1} & \ldots & \ldots & b_{H,H} \end{bmatrix} \quad (7)$$

As an example, let us assume that a PU operates at frequency f_2, where $\mathbf{T}_i$ is transmitted according to (3). Then it is very likely that the received code matrix $\mathbf{R}_n$ will have an all-1 row corresponding to f_2 as:

$$\mathbf{R_n} = \begin{bmatrix} 0 & 1 & 0 \\ 1 & 1 & 1 \\ 0 & 0 & 1 \end{bmatrix} \quad (8)$$

The permutation trellis decoder compares the received code matrix with each of the possible transmitted code matrices, and decides in favor of the symbol whose transmitted code matrix has the minimum Hamming distance with the received code matrix [15].

B. Probability Of Error

We assume that equally-likely M-ary symbols are to be transmitted. So, the average probability of symbol error is given as:

$$P_s = \frac{1}{M}\sum_{i=1}^{M} P_s(\mathbf{T}_i) \quad (9)$$

where $P_s(\mathbf{T}_i)$ is the probability that an individual symbol is received in error. The bit error rate, P_e, is evaluated accordingly,

$$P_e = \frac{\frac{M}{2}}{M-1}.P_s \quad (10)$$

From (9), we calculate the probability that a code matrix $\mathbf{T}_i$ is received in error as:

$$\begin{aligned} P_s(\mathbf{T}_i) &= 1 - P_c(\mathbf{T}_i) \\ &= 1 - \sum_{n=1}^{2^{H^2}} P(\mathbf{D} = \mathbf{T}_i|\mathbf{R}_n)\cdot P(\mathbf{R}_n|\mathbf{T} = \mathbf{T}_i) \quad (11) \end{aligned}$$

where $P_c(\mathbf{T}_i)$ is the probability that symbol i, $i \in \{1,\ldots,M\}$ is received correctly. Let $\mathbf{D}$ be the code matrix which has the minimum Hamming distance with the received code matrix $\mathbf{R}_n$. Then, $P(\mathbf{D} = \mathbf{T}_i|\mathbf{R}_n)$ is the probability that a correct decision has been made given $\mathbf{T}_i$ is the transmitted code matrix. The term $P(\mathbf{R}_n|\mathbf{T} = \mathbf{T}_i)$, is the likelihood and can be written as follows:

$$P(\mathbf{R}_n|\mathbf{T} = \mathbf{T}_i) = \quad (12)$$
$$\prod_{j=1}^{H}\prod_{k=1}^{H}\left\{\prod_{u}^{\mathcal{U}} P(l_{j,k} \geq l_{th}|q_{j,k})\right\}\left\{\prod_{v}^{\mathcal{V}} P(l_{j,k} < l_{th}|q_{j,k})\right\}$$

where $\mathcal{U}$ and $\mathcal{V}$ are the total number of 1's and 0's in the received code matrix $\mathbf{R}_n$. We need to consider two scenarios to compute the probability in (12). The first one considers no PU activity while SU is transmitting and the second scenario considers PU activity on frequency j while SU is transmitting.

1) Absence of PU Activity: Suppose there is no PU transmission in the CRN. Then, the signal received at the input of the envelope detector, $l_{j,k}$, is given by (6). If $q_{j,k} = 1$, then $x_{I_{j,k}} \sim N(\sqrt{E_s}\cos\theta, \frac{N_0}{2})$ and $x_{Q_{j,k}} \sim N(\sqrt{E_s^r}\sin\theta, \frac{N_0}{2})$. Thus, $l_{j,k} \sim Rice(\sqrt{E_s^r}, \sqrt{N_0/2})$. $P(l_{j,k} < l_{th}|q_{j,k} = 1)$ and $P(l_{j,k} \geq l_{th}|q_{j,k} = 1)$ can be computed according to,

$$\begin{aligned} P(l_{j,k} < l_{th}|q_{j,k} = 1) &= F_{L_{j,k}}(l_{th}) \quad (13) \\ &= 1 - Q_1(\sqrt{2E_s^r/N_0}, 0.6\sqrt{2E_s^r/N_0}) \end{aligned}$$

where $F_{L_{j,k}}(l_{th})$ is the cumulative distribution function of $l_{j,k}$ evaluated at l_{th} and

$$P(l_{j,k} \geq l_{th}|q_{j,k} = 1) = 1 - P(l_{j,k} < l_{th}|q_{j,k} = 1) \quad (14)$$

and $Q_1(v,w)$ is the Marcum's Q-function defined as follows:

$$Q_1(v,w) = \int_w^\infty x\exp\left\{-\frac{x^2+v^2}{2}\right\} I_0(vx)\,dx \quad (15)$$

where $I_0(vx)$ is the zeroth order modified bessel function. If $q_{j,k} = 0$, then $x_{I_{j,k}} \sim N(0, \frac{N_0}{2})$ and $x_{Q_{j,k}} \sim N(0, \frac{N_0}{2})$. Consequently, $l_{j,k} \sim Rayleigh(\sqrt{N_0/2})$. $P(l_{j,k} < l_{th}|q_{j,k} = 0)$ and $P(l_{j,k} \geq l_{th}|q_{j,k} = 0)$ can be computed as,

$$\begin{aligned} P(l_{j,k} < l_{th}|q_{j,k} = 0) &= F_{L_{j,k}}(l_{th}) \\ &= 1 - \exp(-0.36E_s^r/N_0) \quad (16) \end{aligned}$$

and

$$P(l_{j,k} \geq l_{th}|q_{j,k} = 0) = 1 - P(l_{j,k} < l_{th}|q_{j,k} = 0) \quad (17)$$

2) Presence of PU Activity: If $q_{j,k} = 1$, the signal received at the input of the demodulator has two significant terms besides noise. One corresponds to the actual signal energy of the transmitted symbol and the other is created by the PU activity, $i_{PU}^r(t)$. It was assumed earlier that the SU transmitting power is low so that QoS of the PU session is maintained. So, the SU signal becomes negligible as compared to that of the PU. Then, $x_{I_{j,k}} \sim N(\sqrt{I_{PU}}\cos\phi, \frac{N_0}{2})$ and $x_{Q_{j,k}} \sim N(\sqrt{I_{PU}}\sin\phi, \frac{N_0}{2})$. Thus, $l_{j,k} \sim Rice(\sqrt{I_{PU}}, \sqrt{N_0/2})$. $P(l_{j,k} < l_{th}|q_{j,k} = 1)$ and $P(l_{j,k} \geq l_{th}|q_{j,k} = 1)$ in the presence of PU activity are calculated as follows:

$$\begin{aligned} &P(l_{j,k} < l_{th}|q_{j,k} = 1) = F_{L_{j,k}}(l_{th}) \\ &= 1 - Q_1(\sqrt{2I_{PU}/N_0}, 0.6\sqrt{2E_s^r/N_0}) \quad (18) \end{aligned}$$

and

$$P(l_{j,k} \geq l_{th}|q_{j,k} = 1) = 1 - P(l_{j,k} < l_{th}|q_{j,k}) \quad (19)$$

If $q_{j,k} = 0$,i.e., the SU does not transmit on subchannel j at time k, the output of the demodulator has the noisy signal received from the PU. In that case, $x_{I_{j,k}} \sim N(\sqrt{I_{PU}}\cos\phi, \frac{N_0}{2})$ and $x_{Q_{j,k}} \sim N(\sqrt{I_{PU}}\sin\phi, \frac{N_0}{2})$. Consequently, $l_{j,k} \sim Rice(\sqrt{I_{PU}}, \sqrt{N_0/2})$. So, the following probabilities $P(l_{j,k} < l_{th}|q_{j,k} = 0)$ and $P(l_{j,k} \geq l_{th}|q_{j,k} = 0)$ are the same as (18) and (19) respectively. Once the probabilities (13) to (19) are evaluated, we can calculate the likelihood for receiving the code matrix $\mathbf{R}_n$, $1 \leq n \leq 2^{H^2}$ given the transmitted code matrix is T_i, $1 \leq i \leq M$. Illustrative examples are provided in the next section.

III. Numerical Results

In this section, we evaluate the performance of the PTC based M-FSK scheme for SU communications and present some numerical results. We assume one PU transmission and one SU transmission as illustrated in Fig. 1. We select the transmit power of the PU as 1 MW and PU is assumed to be operating at f_2. The transmit power of the SU is varied between $[25\mu W, 4mW]$ and the noise power density is selected as $N_0 = 2.5 \times 10^{-14}$. These values validate the assumption in (2). The distances between the SU transmitter receiver pair and that between the PU transmitter and SU receiver are selected as 10 m, which creates a high interference scenario for the SU link. The minimum frequency of a subchannel, f_1, is selected as 56 Mhz, and the bandwidth spacing between two subchannels is selected as 6 MHz. The parameters' values used in the simulation are chosen in accordance with the IEEE 802.22 standard [19].

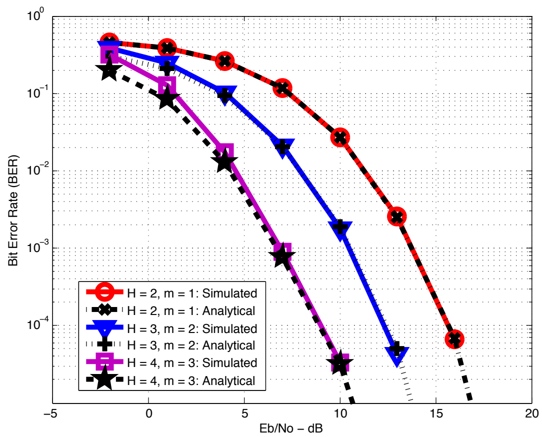

Fig. 3: BER performance of the H-FSK system.

In Fig. 3, we present the BER performance of PTC based M-FSK system as a function of E_b/N_0 for different PTC schemes for $H = \{2, 3, 4\}$. Both analytical and simulation results are presented which match each other quite well. In a general CRN, given the locations of the PUs, their transmitting powers, their QoS requirements, and the average number of active PUs in the network, an SU can compute the expected BER (eBER) of its link prior to its transmission as,

$$\text{eBER} = \sum_{j=1}^{H} \text{BER}(PU = f_j) P(PU = f_j) \qquad (20)$$

where $BER(PU = f_j)$ is the BER of the SU link given that the PU is operating at frequency f_j and is computed according to the procedure described in the previous section. $P(PU = f_j)$ is the probability that PU operates over f_j and can be selected as $P(f_j) = 1/H$.

We next compare the BER performance of PTC based M-FSK scheme with other M-FSK schemes employing conventional ECC techniques. We consider a PTC code with $H = 4$ and $m = 3$ that transmits 3 information bits over 4 frequency subchannels in 4 time steps. In order to perform a fair comparison with other ECC schemes, we select a rate $3/8$ punctured convolutional encoder which is generated from a standard $1/3$ convolutional code. Using the rate $3/8$ punctured convolutional code, 3 information bits are mapped to 8 coded bits. Using 4-FSK modulation, at each time step a 4-FSK symbol is transmitted over one of the 4 frequency subchannels. The transmission of all 8 coded bits is then completed in 4 time steps. As shown in Fig. 4 and given the PU activity on f_2, the BER performance of the PTC based M-FSK scheme is significantly better than the BER performance of convolutional coded M-FSK system. Note that for non-coherent detection, the convolutional coded system uses the standard M-FSK demodulator which consists of M quadrature receivers generating M envelope values for each frequency. The non-coherent M-FSK demodulator then decides on the frequency which has the largest envelope [12]. If there is a strong PU activity in one of the subchannels, the M-FSK demodulator tends to decide in favor of the subchannel where the PU is operating rather than the subchannel where the information signal is transmitted. This results in a catastrophic failure when standard convolutional codes are used. When the transmit power of the PU is reduced to 0.1 W, the transmitting powers of PU and SU become comparable. As a result, convolutional coded SU transmissions can start mitigating the PU interference. However, such a scheme would not be practical since the transmitting power of the SU might violate the QoS requirements of the ongoing PU communication. Following the same procedure of comparison shown above, we use a rate $1/2$ LDPC encoding with a 4-FSK modulation system. Fig. 5 shows how the proposed H-FSK approach also outperforms LDPC codes coupled with an M-FSK modulation scheme.

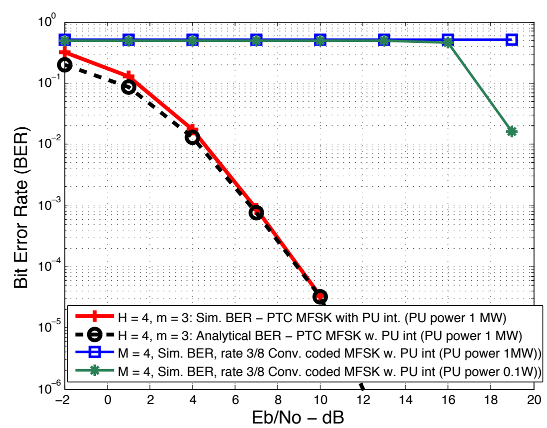

Fig. 4: Performance of PTC based MFSK and Conv. codes under narrowband PU interference.

IV. Conclusion and Future Work

In this paper, we have derived the probability of error of the permutation trellis coded FSK scheme in a cognitive radio context and have verified our analysis with simulation results. The permutation trellis coded FSK scheme outperforms the

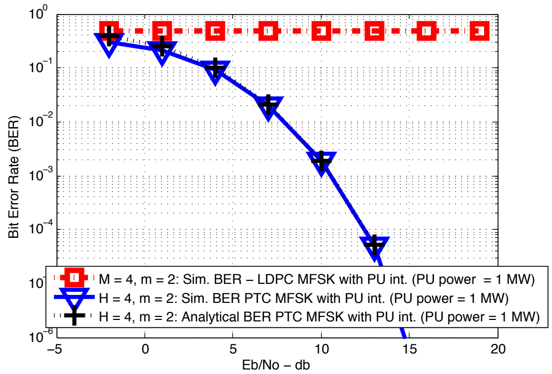

Fig. 5: Performance of PTC based MFSK and LDPC codes under narrowband PU interference.

BER performance of the standard convolutional as well as LDPC coding schemes which is a very promising result when applied in CRNs under heavy PU interference.

In this paper, we assumed that only one PU was active at a given time in the network. If one considers larger number of PUs in the network, H should also be selected to be sufficiently large to provide more resistance to the narrowband interferences caused by the PUs. Note that the complexity of BER computation increases exponentially with H^2, so computationally efficient approximations for the analytical BER are required if it is desired to be used in link adaptation applications. In this work, we evaluated the performance of PTC codes for one SU link only, optimal code assignments in a multi SU scenario will be considered as a future research direction. We will also consider more realistic channel models including shadowing and fading effects.

REFERENCES

[1] I. Akyildiz, W. Lee, M. Vuran, and S. Mohanty, "Next generation/dynamic spectrum access/cognitive radio wireless networks: A survey," *Computer Networks*, vol. 50, no. 13, pp. 2127–2159, 2006.

[2] Q. Zhao and A. Swami, "A decision-theoretic framework for opportunistic spectrum access," *IEEE Transactions on Wireless Communications*, vol. 14, no. 4, pp. 14 –20, Aug. 2007.

[3] S. Haykin, "Cognitive radio: brain-empowered wireless communications," *IEEE Journal on Selected Areas in Communications*, vol. 23, no. 2, pp. 201 – 220, Feb. 2005.

[4] J. Mitola and G. Q. Maguire, "Cognitive radio: making software radios more personal," *IEEE Transactions on Personal Communications*, vol. 6, no. 4, pp. 13 –18, Aug. 1999.

[5] Federal Communications Commission, "Establishment of interference temperature metric to quantify and manage interference and to expand available unlicensed operation in certain fixed mobile and satellite frequency bands," *Et Docket 03-289, Notice of Inquiry and Proposed Rulemaking*, 2003.

[6] T. C. Clancy, "Formalizing the interference temperature model," *Wiley Journal on Wireless Communications and Mobile Computing*, vol. 7, no. 9, pp. 1077–1086, Nov. 2007.

[7] H. Mahmoud, T. Yucek, and H. Arslan, "OFDM for cognitive radio: merits and challenges," *IEEE Transactions on Wireless Communications*, vol. 16, no. 2, pp. 6 –15, April 2009.

[8] F. Shayegh and M. Soleymani, "Rateless codes for cognitive radio in a virtual unlicensed spectrum," in *34th IEEE Sarnoff Symposium*, May 2011, pp. 1 –5.

[9] G. Yue and X. Wang, "Anti-jamming coding techniques with application to cognitive radio," *IEEE Transactions on Wireless Communications*, vol. 8, no. 12, pp. 5996 –6007, December 2009.

[10] J. Ko and C. Kim, "Communication method between spectrum heterogeneous secondary users in ofdm-based cognitive radio," *Electronics Letters*, vol. 47, no. 14, pp. 827 –829, 7 2011.

[11] C. Nicola, H. Mercier, and V. Bhargava, "Error-correcting codes for dynamic spectrum allocation in cognitive radio systems," in *International Symposium on Signals, Systems and Electronics*, August 2007, pp. 247 –250.

[12] J. G. Proakis, *Digital Communications*. McGraw -Hill, 2000.

[13] B. Shahrasbi and N. Rahnavard, "Rateless-coding-based cooperative cognitive radio networks: Design and analysis," in *8th Annual IEEE Conference on Communications Society Sensor, Mesh and Ad Hoc Communications and Networks (SECON), 2011*, June 2011, pp. 224 –232.

[14] W.-C. Ao and K.-C. Chen, "End-to-end HARQ in cognitive radio networks," in *IEEE Wireless Communications and Networking Conference (WCNC)*, April 2010, pp. 1 –6.

[15] H. Ferreira, A. Vinck, T. Swart, and I. de Beer, "Permutation trellis codes," *IEEE Transactions on Communications*, vol. 53, no. 11, pp. 1782 – 1789, Nov. 2005.

[16] T. Swart, I. De Beer, H. Ferreira, and A. Vinck, "Simulation results for permutation trellis codes using M-ary FSK," in *Proc. International Symposium on Power Line Communications and Its Applications,*, April 2005, pp. 317 – 321.

[17] M. Taki and F. Lahouti, "Spectral efficiency optimized adaptive transmission for interfering cognitive radios," in *IEEE International Conference on Communications Workshops*, June 2009, pp. 1 –6.

[18] M. Elalem, L. Zhao, and Z. Liao, "Interference mitigation using power control in cognitive radio networks," in *Proc. IEEE 71st Vehicular Technology Conference*, May 2010, pp. 1 –5.

[19] C. Stevenson, G. Chouinard, Z. Lei, W. Hu, S. Shellhammer, and W. Caldwell, "IEEE 802.22: The first cognitive radio wireless regional area network standard," *IEEE Communications Magazine*, vol. 47, no. 1, pp. 130 –138, January 2009.

ACKNOWLEDGMENT

This material is based on research sponsored in part by CASE: The Center for Advanced Systems and Engineering, a NYSTAR center for advanced technology at Syracuse University.